

# An integrated computational approach for determining the elastic properties of boron nitride nanotubes

V. Vijayaraghavan · A. Garg · C. H. Wong ·  
K. Tai · Pravin M. Singru

Received: 17 March 2014 / Accepted: 27 May 2014 / Published online: 13 June 2014  
© Springer Science+Business Media Dordrecht 2014

**Abstract** An integrated computational approach is proposed to investigate the compressive strength of boron nitride nanotubes (BNNTs). In this approach, an artificial intelligence (AI) cluster comprising of multi-gene genetic programming and molecular dynamics (MD) simulation technique, was specifically designed to formulate the explicit relationship of compressive strength of BNNTs with respect to system aspect ratio (AR), temperature and vacancy defects. It was found that the novel MD based AI model is able to model the compressive strength of BNNTs very well, which is in good agreement with that of experimental results obtained from the literature. Additionally, we also conducted sensitivity and parametric analysis to find out specific influence and variation of each of the input system parameters on the compressive strength of BNNTs. It was found that the AR has the most

dominating influence on the compressive strength of BNNTs.

**Keywords** Mechanical properties · Inorganic compounds · Defects · Nanostructures

## 1 Introduction

Research in boron nitride nanotubes (BNNT) has attracted significant interest in material science due to its attractive physical and mechanical properties (Wang et al. 2010; Griebel and Hamaekers 2007). The exceptional qualities of BNNT has been widely studied and investigated to explore its diverse possible applications in real world. These include applications in electric circuits such as BNNT-based integrated circuits, structural composite materials and hydrogen storage applications (Mohajeri and Omidvar 2014; Yan et al. 2014; Lu et al. 2014). In addition, BNNT is an ideal candidate for potential applications in nano-biological and nano-level drug delivery devices (Ferreira et al. 2013; Del Turco et al. 2013). These applications of BNNT requires a critical understanding of its mechanical properties which are key to design future BNNT based nano-fluidic devices. In addition, the increasing demand to manufacture BNNT based nano-components for electronics industry is one of the major incentives to study the mechanical properties of BNNT.

---

The first two authors contributed equally and are both considered as first authors.

---

V. Vijayaraghavan · A. Garg (✉) · C. H. Wong · K. Tai  
School of Mechanical and Aerospace Engineering,  
Nanyang Technological University, 50 Nanyang Avenue,  
Singapore 639798, Singapore  
e-mail: akhill1@e.ntu.edu.sg

P. M. Singru  
Department of Mechanical Engineering, Birla Institute of  
Technology and Science, BITS Pilani, K.K. Birla Goa  
Campus, Zuarinagar 403726, Goa, India

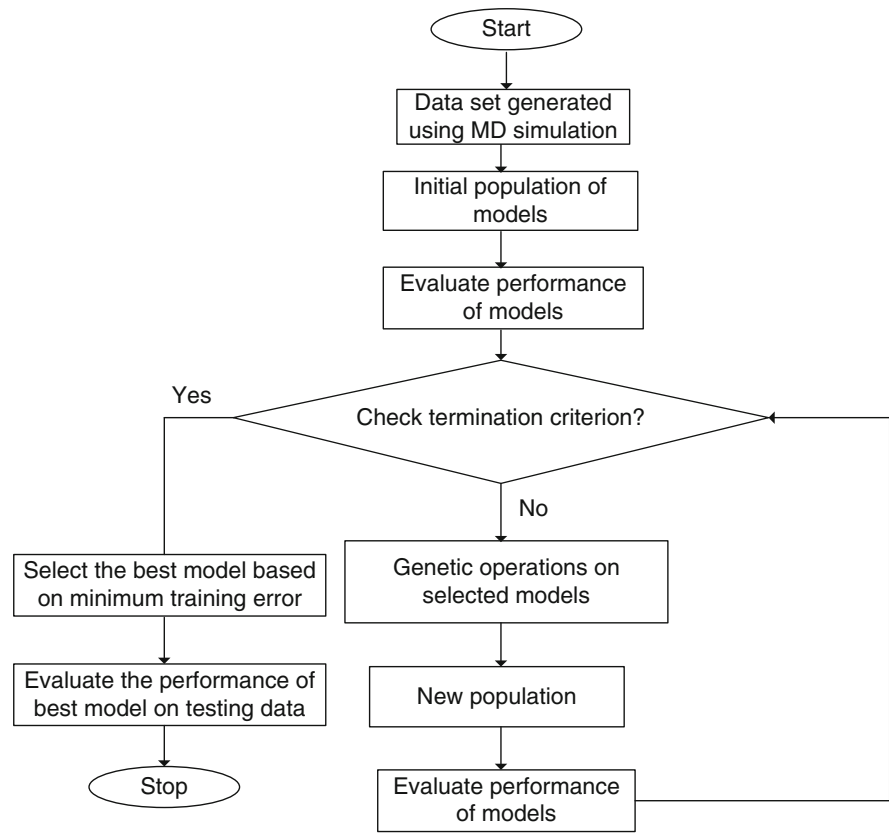
Numerous studies have been undertaken to predict the mechanical properties of BNNT using experimental and computational techniques. Tang et al. (2011) determined the mechanical properties of BNNT under tension using in situ transmission electron microscopy and molecular dynamics (MD) simulation approach. They found that the mechanical properties and deformation behaviors are correlated with the interfacial structure under atomic resolution, which clearly demonstrates a geometry strengthening effect. Liew and Yuan (2011) studied the structural performance of double-walled BNNT under compression at high temperatures using computational modeling approach. They found that the compressive strength and thermal stability of BNNTs are superior to carbon nanotubes (CNT). Shokuhfar et al. (2012) studied the buckling strength of BNNTs at various temperatures using MD simulation technique. They found that the buckling strength generally decreases at high temperatures. Furthermore, the buckling resistance of BNNT was also found to decrease with increasing the length of BNNT. The effect of vacancy defects on the structural properties of BNNT were studied by Ebrahimi-Nejad et al. (2013). It was found from their analysis that the compressive strength of BNNT decreases with increasing vacancy defect concentration in BNNT structure. The compressive strength of BNNT for hydrogen storage applications was analyzed by Ebrahimi-Nejad and Shokuhfar (2013). They found that hydrogen storage decreases the room temperature buckling strength of BNNT. The above mentioned literature studies clearly indicate that the compressive strength of BNNTs depends on various factors such as system size, chirality, temperature and defects. Hence, understanding the influence of each factor on the compressive strength of BNNTs is important for optimizing the elastic properties of BNNT. One way of optimizing system properties of nanoscale materials is to form an explicit model formulation which can then be used to extract system input variables for desirable material performance.

Theoretical studies based on MD simulation has become more popular to study the compressive strength of BNNTs when compared to that of laboratory based experiments. This is due to the reason that MD simulation allows rapid reconstruction of defects, altering of chirality and system size (Wong and Vijayaraghavan 2012a). This is useful to understand

the influence of system parameters on the mechanical properties of BNNT. Hence, MD simulation models can be used as a viable alternative compared to time consuming and expensive experiments for estimating mechanical properties at nanoscale (Vijayaraghavan et al. 2013a, b, 2014; Vijayaraghavan and Wong 2013a, b). In addition, MD simulation is capable of generating accurate solutions in predicting mechanical and thermal properties of nanoscale system with minimal cost and high rapidity (Vijayaraghavan and Wong 2013c, d, 2014; Wong and Vijayaraghavan 2012b, 2014). However, the MD simulation does not provide information on relationship between the input parameters and the generated output. Artificial intelligence (AI) techniques can prove to be a useful tool for predicting the relationship between the input parameters and generated output. However, they cannot be used to predict system properties in nanoscale materials. Additionally, several novel approaches of soft computing methods have been proposed such as hybridizing differential evolution algorithm with receptor editing property of immune system (Yildiz 2012, 2013a, b), artificial bee colony algorithm with Taguchi's method (Yildiz 2013c, d), differential algorithm with Taguchi's method (Yildiz 2013e), cuckoo search algorithm (Yildiz 2013f) and immune algorithm with hill climbing local search algorithm (Yildiz 2009a, b) to optimize the performance characteristics of the materials.

Therefore, there is a need to develop an integrated MD based AI simulation technique for modeling the material properties of nanoscale materials such as BNNT. The new integrated approach combines powerful advantages of accuracy and low cost of MD simulation with the explicit model formulation of AI techniques. These methods require input training data which can be obtained from the MD simulations which is based on a specific geometry and temperature. Considering input data, the AI technique can then be able to generate meaningful solutions for the complicated problems (Vijayaraghavan et al. 2013a, b). Additionally, among the various available AI techniques, an evolutionary approach, namely, Multi-Gene Genetic Programming (MGGP) offers the advantage of a fast and cost-effective explicit formulation of a mathematical model based on multiple variables with no existing analytical models (Cevik et al. 2010; Gandomi and Alavi 2011). It is to the best of author's knowledge that limited or no work exists

**Fig. 1** Mechanism of MD based AI approach for modelling compressive strength of BNNTs



on the application of AI based MD simulation model on evaluating mechanical properties of the nanoscale system. Additionally, the potential future applications of BNNT in electronics industry require a thorough understanding and investigation of various input parameters on the compressive strength of BNNT. Hence, the main purpose of the present study is to investigate the compressive strength of BNNT. The proposed MD based AI approach is employed to investigate the effect of aspect ratio (AR), temperature and vacancy defects on the compressive strength of BNNT. The functional expression (model) of compressive strength with respect to AR, temperature and vacancy defects is obtained. The performance of the proposed model is evaluated against the actual data obtained from literature. Further the parametric and sensitivity analyses conducted is used to validate the robustness of the proposed model by unveiling important hidden parameters and non-linear relationships.

## 2 Integrated MD based AI computational model

The compressive characteristics of BNNTs described in this work is modeled entirely using an integrated MD based AI simulation approach as shown in Fig. 1. In this approach, the MD is integrated in the paradigm of popular AI method, MGGP. For understanding the notion of an integrated approach, each of MD and MGGP method is discussed in the following.

The empirical Tersoff (1988) potential is used to model the compressive characteristics of BNNT based on potential parameters for describing the covalent bonding of boron and nitride atoms developed by Albe et al. (1997) and Albe and Möller (1998). These potential parameters are determined from experimental studies involving impact of nitrogen on hexagonal boron nitride target (Zhang et al. 2009a) and ion-beam deposition on boron nitride thin films (Zhang et al. 2008). The Tersoff potential is described mathematically as,

$$E_{Tersoff} = \frac{1}{2} \sum_i \sum_{i \neq j} f_{cut}(r_{ij}) [A_{ij}f_R(r_{ij}) - B_{ij}f_A(r_{ij})] \quad (1)$$

where  $r_{ij}$  represents scalar distance between the atoms  $i$  and  $j$ ,  $f_{cut}(r_{ij})$  represents the cutoff function,  $f_R$  and  $f_A$  denotes the repulsive and attractive pair terms respectively. The  $A_{ij}$  and  $B_{ij}$  terms are used to include the Tersoff empirical bond order between the atoms.

The data obtained from the MD simulation is further fed into MGGP cluster. The key difference between GP and the MGGP is that, in the latter, the model participating in the evolution is a combination of several sets of genes/trees. GP based on Darwin's theory of 'survival of the fittest' finds the optimal solution by mimicking the process of evolution in nature Koza (1994). Due to which, MGGP has been extensively applied for solving symbolic regression problems of various systems (Garg et al. 2014a, b, c, d).

The initial population of models is obtained by randomly combining the elements from the function and terminal sets. The elements in the function set can be arithmetic operators (+, −, /, ×), non-linear functions (sin, cos, tan, exp, tanh, log) or Boolean operators. The elements of the terminal set are input process variables and random constants. The present study has three input process variables, and, therefore these are chosen as elements of terminal set. The constants are chosen randomly in the range as specified by the user since these accounts for the human or experimental error. The performance of the initial population is measured using the fitness function, which compares the predicted values of the MGGP model to that of the actual values. Fitness function must be minimized for obtaining better solutions. Typically used fitness function, namely, root mean square error (RMSE) is given by

$$RMSE = \sqrt{\frac{\sum_{i=1}^N |G_i - A_i|^2}{N}} \quad (2)$$

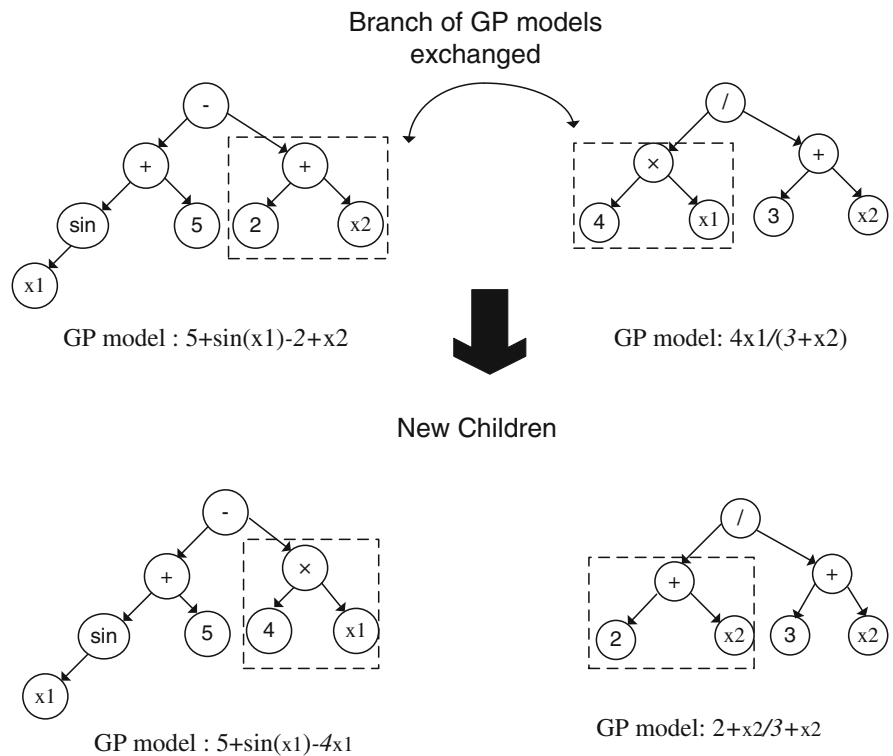
where  $G_i$  is the valued predicted of  $i$ th data sample by the MGGP model,  $A_i$  is the actual value of the  $i$ th data sample and  $N$  is the number of training samples.

The performance of the initial population is evaluated and the termination criterion is checked. The termination criterion is specified by the user and is the maximum number of generations and/or the threshold

error of the model. If the performance does not match the criterion, the new population is generated by performing the genetic operators on the selected individuals of the initial population. Genetic operators applied are crossover, mutation and reproduction. Tournament selection method is used to select the individuals for the genetic operations. This selection method maintains genetic diversity in the population and thus avoids local/premature convergence. Tournament sizes of 2, 4 and 7 are preferred. The models with lowest fitness value reproduce or copied in the next generation. The crossover operation, namely, subtree crossover is used. Figure 2 shows the functioning of subtree crossover in which the branch of the two models is chosen randomly and swapped. The mutation used is subtree mutation (Fig. 3) in which the branch of the model is replaced with the newly randomly generated model/tree. As recommended by Koza (1994), the probability rate of reproduction, crossover and mutation kept is 85, 10 and 5 % respectively. This indicates that most of the new population came from the application of crossover operation. The iterative phenomenon of generating new population continues as long as the termination criterion is met. The best model is selected based on minimum RMSE and its performance is evaluated on testing data.

### 3 Modeling mechanical loading of BNNT structure

The BNNT structure is first thermally equilibrated in an NVT ensemble to release any residual stresses. The simulations are carried out by maintaining the desired system temperature. Six temperatures ranging from 0 to 1,500 K are considered in our study to gather the required data of mechanical strength. The mechanical strength in our study is defined as the maximum compressive force that BNNT structure can sustain under compression. The temperature stability of the system is attained by using the Nose–Hoover thermostat (Hoover 1985; Nose 1984). Following equilibration, the SWCNT is subjected to compressive loading as shown in Fig. 4. It can be seen from Fig. 4 that the end atoms enclosed inside the red rectangle is subjected to a constant inward displacement (strain rate = 0.001 ps<sup>−1</sup>). The system is allowed to relax after every 1,000 time steps such that the atoms attain the favorable minimum energy positions. The inward

**Fig. 2** Subtree crossover operation

velocity and the trajectories of end atoms are calculated and the atoms are subsequently shifted to the new position. The remaining atoms are relaxed in an NVT ensemble and the procedure is repeated until failure occurs. We used a total of 600,000 time steps (including 200,000 time steps for initial equilibration) with each time step equivalent to 1 fs. The snap shot of computer simulation of compressing the BNNT structure is shown in Fig. 5. It can be seen from this figure that when no force is applied, the BNNT maintains its stable structure. However, application of compressive force results in buckling that causes kinks and fins to be formed along the surface of BNNT. Figure 6 shows the variation of the engineering stress of BNNT with strain resulting from our computer simulation. The variation of engineering stress with strain from our simulation model agrees well with the experimental results of Tang et al. (2011) which confirms the accuracy of our study.

The effect of size on mechanical strength of BNNTs is studied by varying the AR (ratio of length to diameter of the BNNT). The diameter of BNNT is varied by changing the chirality of BNNT structure. The effect of temperature is studied by carrying out the

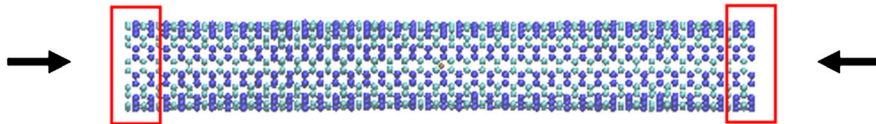
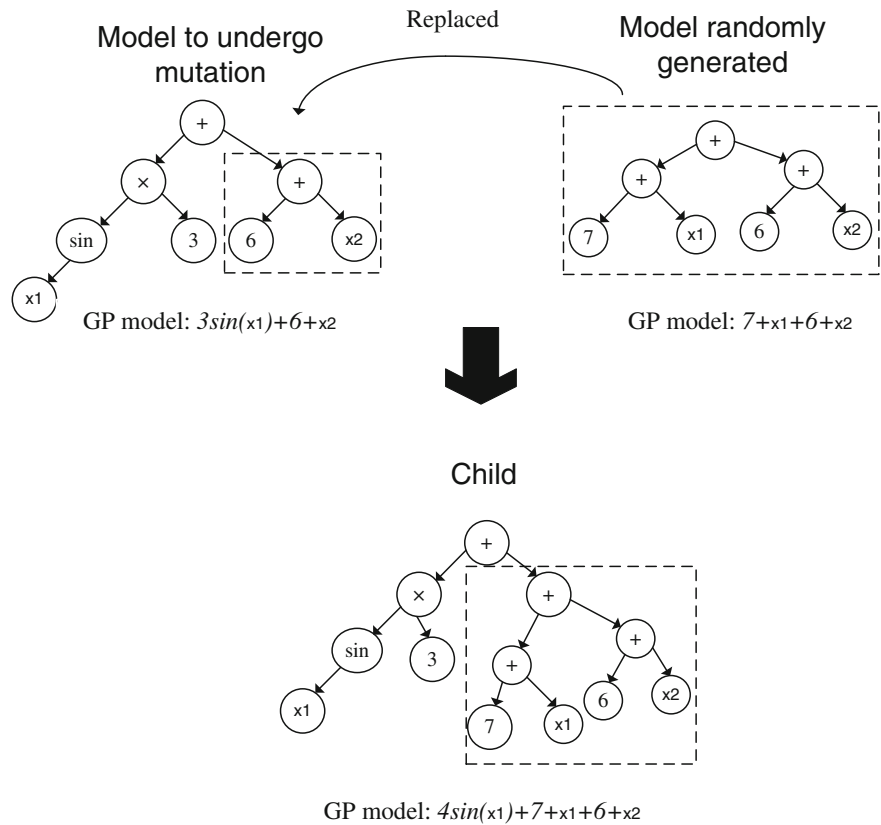
mechanical loading of BNNT at six different temperatures, viz. 0, 300, 600, 900, 1,200 and 1,500 K. The influence of vacancy defects on the mechanical strength of BNNT is studied by manually reconstructing vacancy defects ranging from 1 to 4 missing atoms in the perfect hexagonal lattice of BNNT.

## 4 Results and discussion

### 4.1 Effect of AR of BNNT

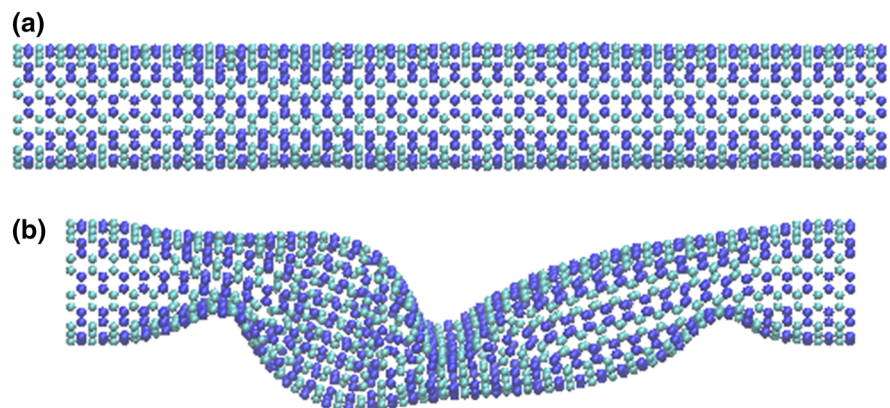
The mechanical strength of BNNTs with various AR is described in this section. As defined in Sect. 3, the measure of mechanical strength is defined by the maximum compressive force that the BNNT can sustain under compression. The variation of maximum compressive force with AR of BNNT is described in Fig. 7. It can be noted from this figure that the maximum compressive force shows a decreasing trend with AR of BNNT which is in perfect agreement with previous studies on compression of nanotubes (Wong and Vijayaraghavan 2014; Liew et al. 2004). This is because for a given diameter, increasing the AR

**Fig. 3** Subtree mutation operation



**Fig. 4** Procedure of mechanical loading of BNNT under compression. The end atoms enclosed within the red colored rectangle is subjected to inward displacement to effect compression. (Color figure online)

**Fig. 5** Snap shot of mechanical testing of BNNT under compression. The BNNT maintains a stable structure at strain  $\varepsilon = 0$  (a), further application of compressive forces results in formation of kinks and fins which distorts the BNNT structure at strain  $\varepsilon = 4.2$  (b)





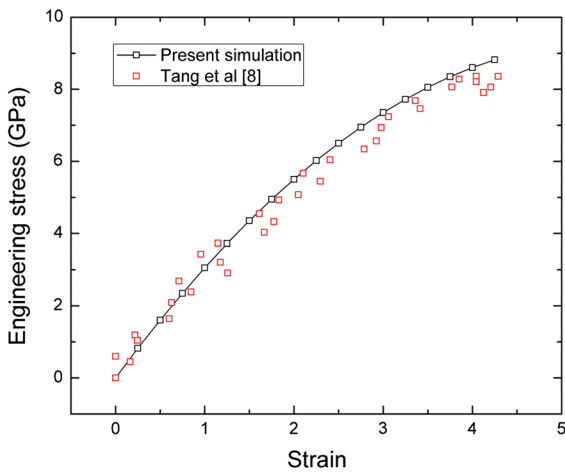


**Fig. 6** Plot showing the variation of engineering stress with strain of BNNT. The data obtained from our computer simulation agrees well with experimental data of Tang et al. (2011) validating the accuracy of our simulation model

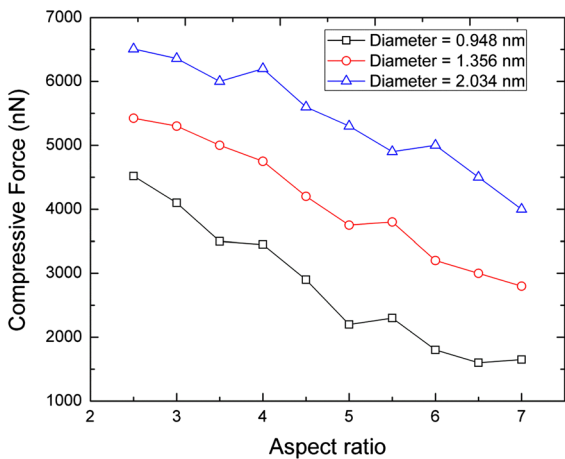


**Fig. 7** Compressive force of BNNTs with various ARs at temperature,  $T = 0$  K. The data is grouped based on the diameter of BNNT

increases the length of BNNT. Hence BNNTs with higher ARs are comparatively more slender to that of small AR stocky BNNTs. The slenderness will result in lateral bending of the BNNT structure which decreases the ability of BNNT to withstand pure axial compression. Additionally, we note that bigger BNNTs can sustain large compressive force compared to small diameter BNNT. This could be explained due to the reason that increasing the diameter results in an increase in cross-sectional area of BNNT that improves the compression characteristic of BNNT.

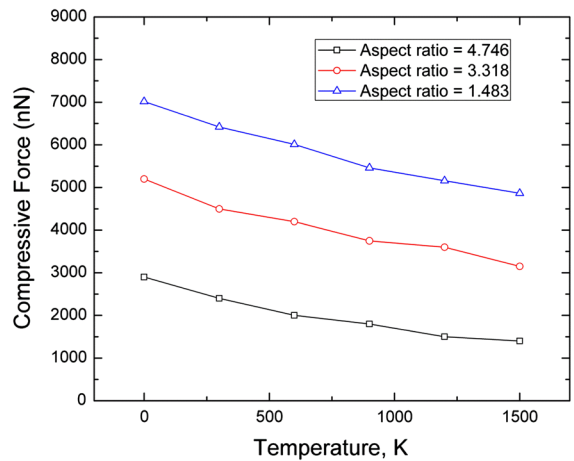


**Fig. 8** Compressive force of BNNTs for temperatures ranging from 0 to 1,500 K. The data is grouped based on the AR of BNNT

#### 4.2 Effect of temperature

The effect of temperature on the mechanical strength of BNNTs is also studied in our work. The effect of temperature is considered by varying the simulation temperature from  $T = 0$  K to  $T = 1,500$  K in steps of 300 K. The variation of maximum compressive force of BNNT with temperatures for various ARs is shown in Fig. 8. We note from this figure that the mechanical strength of BNNTs decreases with increasing temperature. This is due to the reason that increasing the temperature of BNNT will result in greater thermal vibration of atoms which correspondingly increases the thermal stress of BNNT. This increase in thermal stress will in turn decrease the compressive characteristics of BNNT. Additionally, the percentage decrease in compressive force of BNNT due to increase in temperature with varying ARs is listed in Table 1. We see from this table that a bigger BNNT (i.e. with small AR) is more sensitive to temperature compared to that of a smaller BNNT (i.e. with large AR). This phenomenon as explained by Zhang and Shen (2007) is probably due to reason that the onset of buckling is caused by perturbations and disturbances along the tube wall of BNNT. Increasing the temperature will result in larger amplitude of thermal oscillations that correspondingly results in wide disturbances over a large surface area (in BNNTs with large tube diameter) which assists in faster buckling of bigger BNNTs.

**Table 1** Percentage decrease in compressive force due to increasing temperature from  $T = 0$  K to  $T = 1,500$  K for select ARs of BNNT

Aspect ratio	Percentage decrease in compressive force of BNNT due to increasing temperature from $T = 0$ K to $T = 1,500$ K
4.746	51.72
3.318	39.42
1.483	30.65

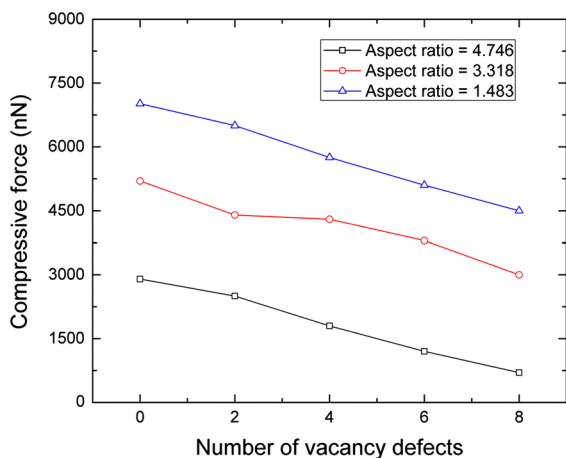


**Fig. 9** Compressive force of BNNTs of select ARs with varying vacancy defect concentrations at temperature,  $T = 0$  K

#### 4.3 Effect of vacancy defects

The effect of defects on the mechanical strength of BNNT is taken into account by constructing vacancy defects in the geometry of BNNT. The variation of compressive force of BNNTs with varying vacancy concentrations is shown in Fig. 9. The compressive force of BNNT decreases with increasing vacancy defect concentration in BNNT. The variation of compressive force with vacancy defects predicted from our study is in qualitative agreement with previous studies on compressive characteristics of nanotubes (Zhang et al. 2009; Wong 2010). We also note from Fig. 9 that smaller BNNTs are more susceptible to vacancy defects compared to that of bigger BNNTs. This is because the vacancy defect

occupies a much larger surface area in smaller BNNT compared to that of bigger BNNTs. This increase in surface area results in lesser number of bonds which can hold the structure of BNNT. This ultimately results in larger drop in the compressive force of BNNT.

#### 4.4 Description of data

Data obtained from the MD simulations comprise of three input process variables i.e., AR of BNNTs ( $x_1$ ), temperature ( $x_2$ ), number of vacancy defects ( $x_3$ ) and the one output process variable, namely, the compressive strength ( $y_1$ ). 47 data points for BNNTs are obtained from the MD simulations as discussed in Sects. 4.1 and 4.2. Nature of the data points collected is shown in Table 2. Selection of the training samples affect the learning phenomenon of the proposed model. In this work, 80 % of the total samples are chosen randomly as training samples with the remaining used as the set of the test samples. Data is then fed into cluster of the proposed model.

In the present work, GPTIPS (Hinchliffe et al. 1996; Searson et al. 2010) is used to perform the implementation of proposed approach for the evaluation of compressive strength of BNNTs. Several applications of this approach is discussed (Garg et al. 2014e, f, g, h; Garg and Tai 2013). Approach is applied to the data set as shown in Table 1. For the effective implementation of the proposed approach, the parameter settings are adjusted using the trial-and-error method (see Table 3). Wide range of elements is chosen in the function set so as to generate the mathematical models of different sizes. Depending on the problem, the values of population size and generations are set. The size and variety of forms of the model to be searched in the solution space is determined by the maximum number of genes and depth of the gene. Based on collection of good number of data samples for the BNNTs, the maximum number of genes and maximum depth of gene is chosen at 8 and 6 respectively. The performance of the best model (see Eq. 3) selected is shown in the following section. In this model,  $x_1$ ,  $x_2$  and  $x_3$  are AR, temperature and number of vacancy defects for the BNNTs.



$$\begin{aligned}
 \text{MD\_AI\_Model} = & 7075.9395 + (0.15325) * ((\exp((4.751686))) + (\exp(\text{plog}(x_2)))) \\
 & + (29.9508) * ((\tan(\cos(\text{plog}(x_2)))) + (\text{plog}((\cos(\exp(x_3))) - (\sin((x_3) + (x_1)))))) \\
 & + (-0.010533) * (((\exp(x_3)) * ((\cos(\exp(x_3))) - (\sin((4.798872)))))) * ((\cos(x_3)) - (\sin((4.798872)))) \\
 & + (-59.0461) * (((x_1) * (x_1)) * (\tan((4.428378)))) \\
 & + (-53.8336) * (\text{plog}(\text{plog}((\cos(\exp(x_3))) - (\cos((x_3) + (x_1)))))) \\
 & + (-85.7442) * (((x_3) + ((x_3) - (x_1))) + (x_3)) \\
 & + (-242.8619) * (\tanh(\text{plog}((\cos(\exp(x_3))) - (\sin((x_3) + (x_1)))))) \\
 & + (61.3814) * ((\sin((x_3) + (x_1))) - (\sin(((x_3) + (x_1)) + (x_1)))) \tag{3}
 \end{aligned}$$

**Table 2** Descriptive statistics of the input and output process variables obtained from MD simulations for BNNTs

Statistical parameter	Aspect ratio ( $x_1$ )	Temperature ( $x_2$ )	Number of vacancy defects ( $x_3$ )	Compressive strength ( $y$ )
Mean	3.04	627.65	5.36	3,562.38
Standard error	0.19	64.98	0.50	280.88
Median	3.31	550	6	4,271.71
Standard deviation	1.36	445.48	3.46	1,925.63
Variance	1.85	198,457.44	12.01	3.70
Kurtosis	-1.59	-0.86	-1.02	-0.85
Skewness	0.01	0.47	-0.10	-0.26
Minimum	1.48	0	0	61.00
Maximum	4.74	1,500	12	7,016

**Table 3** Parameter settings for proposed MD based AI model

Parameters	Values assigned
Runs	8
Population size	100
Number of generations	100
Tournament size	3
Max depth of tree	6
Max genes	8
Functional set (F)	(Multiply, plus, minus, plog, tan, tanh, sin, cos exp)
Terminal set (T)	( $x_1, x_2, x_3, [-10 \ 10]$ )
Crossover probability rate	0.85
Reproduction probability rate	0.10
Mutation probability rate	0.05

4.5 Performance evaluation of proposed MD based AI model to that of actual results

The results obtained from the MD based AI model is illustrated in Fig. 10 on the training and testing data.

Performance of the proposed model is evaluated against the actual results of Ebrahimi-Nejad and Shokuhfar (2013) using the five metrics: the square of the correlation coefficient ( $R^2$ ), the mean absolute percentage error (MAPE), the RMSE, relative error (%) and multi-objective error function (MO) given by

$$R^2 = \left( \frac{\sum_{i=1}^n (A_i - \bar{A}_i)(M_i - \bar{M}_i)}{\sqrt{\sum_{i=1}^n (A_i - \bar{A}_i)^2 \sum_{i=1}^n (M_i - \bar{M}_i)^2}} \right)^2 \tag{4}$$

$$\text{MAPE} (\%) = \frac{1}{n} \sum_i \left| \frac{A_i - M_i}{A_i} \right| \times 100 \tag{5}$$

$$\text{RMSE} = \sqrt{\frac{\sum_{i=1}^N |M_i - A_i|^2}{N}} \tag{6}$$

$$\text{Relative error} (\%) = \frac{|M_i - A_i|}{A_i} \times 100 \tag{7}$$

$$\text{Multiobjective error} = \frac{\text{MAPE} + \text{RMSE}}{R^2} \tag{8}$$

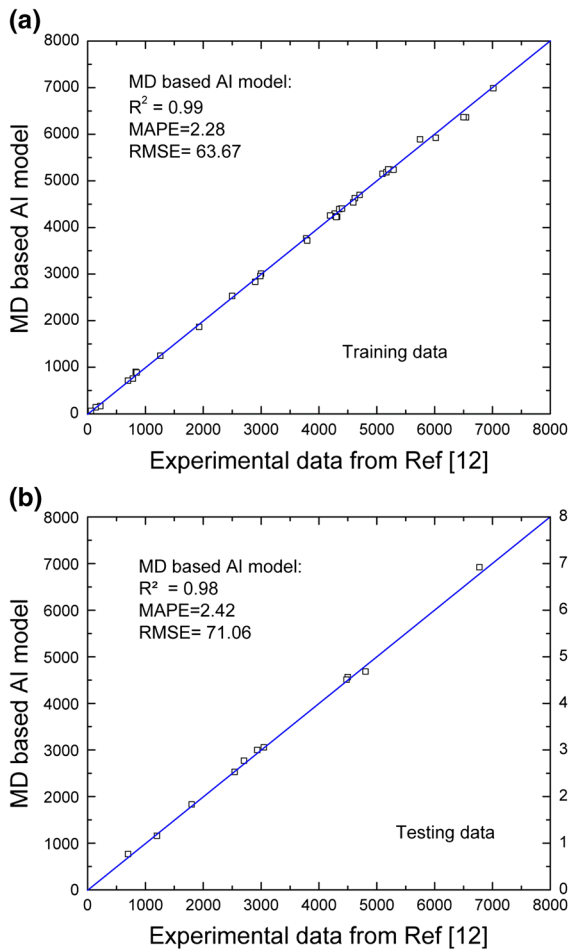


**Fig. 10** Performance of the MD based AI model for the BNNTs on training and testing data

**Table 4** Multi-objective error of the MD based AI model

MD based AI model	Training data	Testing data
BNNTs	54.84	59.25

where  $M_i$  and  $A_i$  are the predicted and actual values respectively,  $M_i$  and  $A_i$  are the average values of the predicted and actual respectively and  $n$  is the number of training samples. Since, the values of  $R^2$  do not change by changing the models values equally and the functions:

**Table 5** Descriptive statistics based on the relative error (%) of the MD based AI model

MD based AI model	Count	Mean	LCI 95 %	UCI 95 %	SD	SE mean	Median	Maximum	Minimum
BNNTs	47	2.31	1.16	3.46	3.90	0.56	1.41	25.55	1.41

**Table 6**  $P$  values to evaluate goodness of fit of the MD based AI model

95 % CI	BNNTs
Mean paired $t$ test	0.98
Variance $F$ test	0.97

MAPE, RMSE and relative error only shows the error and no correlation. Therefore, a MO error function that is a combination of these metrics is also used.

The result of the training phase shown in Fig. 10a indicates that the proposed model have impressively learned the non-linear relationship between the input variables and compressive strength with high correlation values and relatively low error values. The result of the testing phase shown in Fig. 10b indicates that the predictions obtained from the MD based AI model are in good agreement with the actual data, with achieved values of  $R^2$  as high as 0.98.

MO values of the proposed model are computed on the training and testing data as shown in Table 4. The descriptive statistics of the relative error of the proposed model are shown in Table 5, which illustrates error mean, standard deviation (SD), standard error of mean (SE mean), lower confidence interval (LCI) of mean at 95 %, upper confidence interval (UCI) of mean at 95 %, median, maximum and minimum. The lower values of range (UCI-LCI) of the confidence intervals of the proposed model indicates that it is able to generalize the compressive strength values satisfactory based on the variations in AR, temperature and incursion of defects.

Goodness of fit of the proposed model is evaluated based on the hypothesis tests and shown in Table 6. These are  $t$  tests to determine the mean and  $f$  tests for variance. For the  $t$  tests and the  $f$  tests, the  $P$  value of the model is  $>0.05$ , so there is not enough evidence to conclude that the actual values and predicted values from the model differ. Therefore, the proposed model has statistically satisfactory goodness of fit from the modeling point of view.

Thus, from the statistical comparison presented, it can be concluded that the proposed MD based AI

model is able to capture the dynamics of the interactive effect of the AR, temperature and the number of defects on the compressive strength of BNNTs.

#### 4.6 Sensitivity and parametric analysis of the MD based AI model

Sensitivity and parametric analysis about the mean is conducted for validating the robustness of our

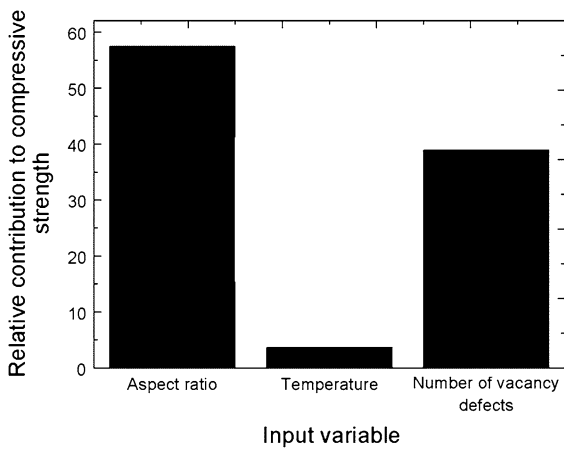
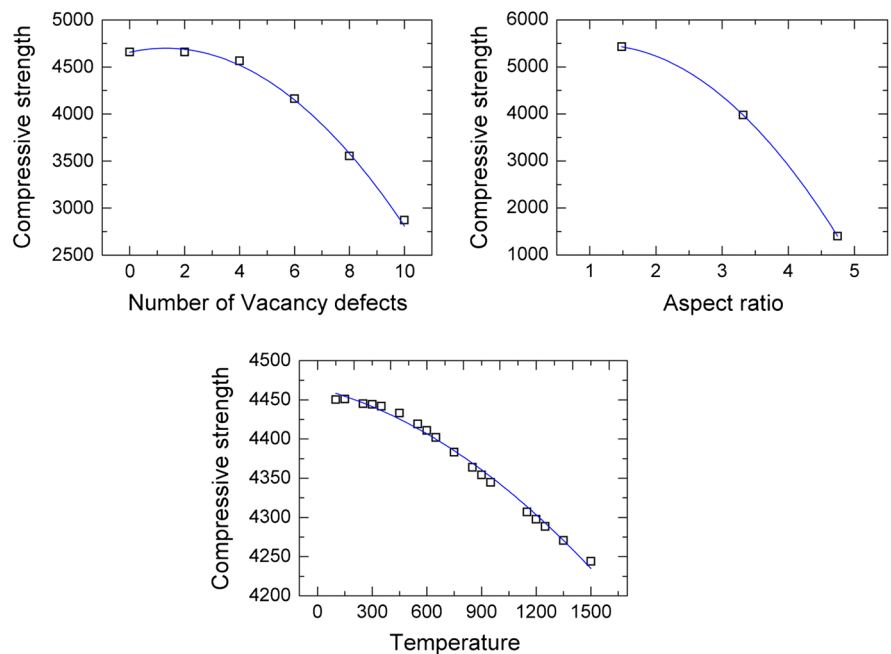


**Fig. 11** Amount of impact of input variables to the compressive strength of BNNT

**Fig. 12** Parametric analysis of the MD based AI model showing the effect of variation of compressive strength in respect to input variables for BNNT



proposed MD based AI model. The sensitivity analysis (SA) percentage of the output to each input parameter is determined using the following formulas:

$$L_i = f_{\max}(x_i) - f_{\min}(x_i) \tag{9}$$

$$SA_i = \frac{L_i}{\sum_{j=1}^n L_j} \times 100 \tag{10}$$

where  $f_{\max}(x_i)$  and  $f_{\min}(x_i)$  are, respectively, the maximum and minimum of the predicted output over the  $i$ th input domain, where the other variables are equal to their mean values.

Figure 11 shows the plots of the sensitivity results of input variables in the prediction of compressive strength of BNNTs. From Fig. 11a, b, it is clear that the process input variable, namely the AR, has the greater impact on the compressive strength of BNNTs followed by number of defects and temperature. This reveals that by regulating the AR of BNNTs, a greatest variation in compressive strength of BNNTs can be achieved. The parametric analysis provides a measure of the relative importance among the inputs of the model and illustrates how the compressive strength of BNNTs varies in response to the variation in input variables. For this reason, on the formulated MD based AI model, the first input is varied between its mean  $\pm$  definite number of SDs, and the compressive strength is computed, while, the other input is fixed at

its mean value. This analysis is then repeated for the other inputs. Figure 12 displays the plots generated for each input variable and the compressive strength of BNNTs. These plots reveal that, for example, the compressive strength decreases with an increase in all three input variables. The analysis complies well in agreement with that of studies conducted by Ebrahimi-Nejad and Shokuhfar (2013). From the Fig. 12, we can then select the optimal values of the input variables, which optimises the compressive strength. In this way, our proposed MD based AI model can be used to reveals insights on the phenomenon of impact on the compressive strength with variations in AR, temperature and number of defects.

## 5 Conclusions

The present work discusses the experimental and MD based studies conducted for the evaluation of compressive strength of nanoscale materials. Alternatively, we proposed the MD based AI approach and explored its ability in simulating the compressive strength characteristic of BNNTs based on AR, temperature and number of defects. The results show that the predictions obtained from the proposed model are in good agreement with the actual data of Ebrahimi-Nejad and Shokuhfar (2013). Based on the sensitivity and parametric analysis, the important process parameters and the hidden non-linear relationships are unveiled, which further validate the robustness of our proposed model. The higher generalization ability of the proposed model obtained is beneficial for experts in evaluation of compressive strength in uncertain input process conditions. An MD based AI method evolve model (see Eq. 3) that represents the explicit formulation between the compressive strength and input process parameters. Thus, by using the MD based AI model, the vital economic factors such as time and cost for estimating the compressive strength using the trial-and-error experimental approach can be reduced.

The present work illustrates the use of proposed approach to compute the effect of AR, temperature and number of defects on the compressive strength of BNNTs. The significance of the work includes the development of explicit mathematical formulation, which could be used by engineers for estimating the compressive strength based on AR, temperature and

number of defects, and in-turn, will be useful for their design purposes. However, further work is needed to estimate the compressive strength for the other types of hybridized BNNTs and graphene structures and their interactions with water and evaluate any differences to those of the current study.

**Acknowledgments** This work was partially supported by the Singapore Ministry of Education Academic Research Fund through Research Grant RG30/10, which the authors gratefully acknowledge.

## References

- Albe, K., Möller, W.: Modelling of boron nitride: atomic scale simulations on thin film growth. *Comput. Mater. Sci.* **10**(1–4), 111–115 (1998)
- Albe, K., Möller, W., Heinig, K.-H.: Computer simulation and boron nitride. *Radiat. Eff. Defects Solids* **141**(1–4), 85–97 (1997)
- Cevik, A., et al.: Soft computing based formulation for strength enhancement of CFRP confined concrete cylinders. *Adv. Eng. Softw.* **41**(4), 527–536 (2010)
- Del Turco, S., et al.: Cytocompatibility evaluation of glycol-chitosan coated boron nitride nanotubes in human endothelial cells. *Colloids Surf. B* **111**, 142–149 (2013)
- Ebrahimi-Nejad, S., Shokuhfar, A.: Compressive buckling of open-ended boron nitride nanotubes in hydrogen storage applications. *Physica E* **50**, 29–36 (2013)
- Ebrahimi-Nejad, S., et al.: Effects of structural defects on the compressive buckling of boron nitride nanotubes. *Physica E* **48**, 53–60 (2013)
- Ferreira, T.H., et al.: Boron nitride nanotubes coated with organic hydrophilic agents: stability and cytocompatibility studies. *Mater. Sci. Eng. C* **33**(8), 4616–4623 (2013)
- Gandomi, A.H., Alavi, A.H.: Multi-stage genetic programming: a new strategy to nonlinear system modeling. *Inf. Sci.* **181**(23), 5227–5239 (2011)
- Garg, A., Tai, K.: Genetic programming for modeling vibratory finishing process: role of experimental designs and fitness functions. In: Panigrahi, B.K., Suganthan, P.N., Das, S., Dash, S.S. (eds.) SEMCCO 2013—Proceedings of the 4th International Conference on Swarm, Evolutionary and Memetic Computing—Part II, Chennai, India, 19–21 December 2013, Lecture Notes in Computer Science, vol. 8298, pp. 23–31. Springer (2013)
- Garg, A., et al.: An embedded simulation approach for modeling the thermal conductivity of 2D nanoscale material. *Simul. Model. Pract. Theory* **44**, 1–13 (2014a)
- Garg, A., et al.: Performance evaluation of microbial fuel cell by artificial intelligence methods. *Expert Syst. Appl.* **41**(4), 1389–1399 (2014b)
- Garg, A., Tai, K., Savalani, M.: State-of-the-art in empirical modelling of rapid prototyping processes. *Rapid Prototyping J.* **20**(2), 164–178 (2014c)
- Garg, A., Garg, A., Tai, K.: A multi-gene genetic programming model for estimating stress-dependent soil water retention curves. *Comput. Geosci.* **18**(1), 45–56 (2014d)

- Garg, A., Tai, K., Savalani, M.: Formulation of bead width model of an SLM prototype using modified multi-gene genetic programming approach. *Intl. J. Adv. Manuf. Technol.* (2014e). doi:[10.1007/s00170-014-5820-9](https://doi.org/10.1007/s00170-014-5820-9)
- Garg, A., Tai, K., Gupta, A.: A modified multi-gene genetic programming approach for modelling true stress of dynamic strain aging regime of austenitic stainless steel 304. *Meccanica* **49**(5), 1193–1209 (2014f)
- Garg, A., et al.: Estimation of factor of safety of rooted slope using an evolutionary approach. *Ecol. Eng.* **64**, 314–324 (2014g)
- Garg, A., et al.: An integrated SRM-multi-gene genetic programming approach for prediction of factor of safety of 3-D soil nailed slopes. *Eng. Appl. Artif. Intell.* **30**, 30–40 (2014h)
- Griebel, M., Hamaekers, J.: Molecular dynamics simulations of boron-nitride nanotubes embedded in amorphous Si–B–N. *Comput. Mater. Sci.* **39**(3), 502–517 (2007)
- Hinchliffe, M., et al.: Modelling chemical process systems using a multi-gene genetic programming algorithm. *Late Breaking Paper, Gp'96*. pp. 28–31. Stanford, USA (1996)
- Hoover, W.G.: Canonical dynamics—equilibrium phase-space distributions. *Phys. Rev. A* **31**(3), 1695–1697 (1985)
- Koza, J.R.: Genetic programming as a means for programming computers by natural selection. *Stat. Comput.* **4**(2), 87–112 (1994)
- Liew, K.M., Yuan, J.: High-temperature thermal stability and axial compressive properties of a coaxial carbon nanotube inside a boron nitride nanotube. *Nanotechnology* **22**(8), 085701 (2011)
- Liew, K.M., et al.: Nanomechanics of single and multiwalled carbon nanotubes. *Phys. Rev. B* **69**(11), 115429 (2004)
- Lu, H., Lei, M., Leng, J.: Significantly improving electro-activated shape recovery performance of shape memory nanocomposite by self-assembled carbon nanofiber and hexagonal boron nitride. *J. Appl. Polym. Sci.* (2014). doi:[10.1002/app.40506](https://doi.org/10.1002/app.40506)
- Mohajeri, A., Omidvar, A.: Density functional theory study on the static dipole polarizability of boron nitride nanotubes: single wall and coaxial systems. *J. Phys. Chem. C* **118**(3), 1739–1745 (2014)
- Nose, S.: A unified formulation of the constant temperature molecular-dynamics methods. *J. Chem. Phys.* **81**(1), 511–519 (1984)
- Searson, D.P., Leahy, D.E., Willis, M.J.: GPTIPS: an open source genetic programming toolbox for multigene symbolic regression. In: *Proceedings of the International MultiConference of Engineers and Computer Scientists, Citeseer* (2010)
- Shokuhfar, A., et al.: The effect of temperature on the compressive buckling of boron nitride nanotubes. *Phys. Status Solidi A* **209**(7), 1266–1273 (2012)
- Tang, D.M., et al.: Mechanical properties of bamboo-like boron nitride nanotubes by in situ TEM and MD simulations: strengthening effect of interlocked joint interfaces. *ACS Nano* **5**(9), 7362–7368 (2011)
- Tersoff, J.: New empirical approach for the structure and energy of covalent systems. *Phys. Rev. B* **37**(12), 6991–7000 (1988)
- Vijayaraghavan, V., Wong, C.: Temperature, defect and size effect on the elastic properties of imperfectly straight carbon nanotubes by using molecular dynamics simulation. *Comput. Mater. Sci.* **71**, 184–191 (2013a)
- Vijayaraghavan, V., Wong, C.H.: Shear deformation characteristics of single walled carbon nanotube with water interactions by using molecular dynamics simulation. *Physica E* **54**, 206–213 (2013b)
- Vijayaraghavan, V., Wong, C.H.: Nanomechanics of single walled carbon nanotube with water interactions under axial tension by using molecular dynamics simulation. *Comput. Mater. Sci.* **79**, 519–526 (2013c)
- Vijayaraghavan, V., Wong, C.H.: Temperature, defect and size effect on the elastic properties of imperfectly straight carbon nanotubes by using molecular dynamics simulation. *Comput. Mater. Sci.* **71**, 184–191 (2013d)
- Vijayaraghavan, V., Wong, C.H.: Transport characteristics of water molecules in carbon nanotubes investigated by using molecular dynamics simulation. *Comput. Mater. Sci.* **89**, 36–44 (2014)
- Vijayaraghavan, V., et al.: Estimation of mechanical properties of nanomaterials using artificial intelligence methods. *Appl. Phys. A* (2013a). doi:[10.1007/s00339-013-8192-3](https://doi.org/10.1007/s00339-013-8192-3)
- Vijayaraghavan, V., et al.: Predicting the mechanical characteristics of hydrogen functionalized graphene sheets using artificial neural network approach. *J. Nanostruct. Chem.* **3**(1), 83 (2013b)
- Vijayaraghavan, V., et al.: Measurement of properties of graphene sheets subjected to drilling operation using computer simulation. *Measurement* **50**, 50–62 (2014)
- Wang, J., Lee, C.H., Yap, Y.K.: Recent advancements in boron nitride nanotubes. *Nanoscale* **2**(10), 2028–2034 (2010)
- Wong, C.H.: Elastic properties of imperfect single-walled carbon nanotubes under axial tension. *Comput. Mater. Sci.* **49**(1), 143–147 (2010)
- Wong, C.H., Vijayaraghavan, V.: Nanomechanics of nonideal single- and double-walled carbon nanotubes. *J. Nanomater.* Article ID 490872 (2012a). doi:[10.1155/2012/490872](https://doi.org/10.1155/2012/490872)
- Wong, C.H., Vijayaraghavan, V.: Nanomechanics of free form and water submerged single layer graphene sheet under axial tension by using molecular dynamics simulation. *Mater. Sci. Eng. A* **556**, 420–428 (2012b)
- Wong, C.H., Vijayaraghavan, V.: Compressive characteristics of single walled carbon nanotube with water interactions investigated by using molecular dynamics simulation. *Phys. Lett. A* **378**(5–6), 570–576 (2014)
- Yan, H., et al.: Enhanced thermal-mechanical properties of polymer composites with hybrid boron nitride nanofillers. *Appl. Phys. A* **114**(2), 331–337 (2014)
- Yildiz, A.R.: A novel hybrid immune algorithm for global optimization in design and manufacturing. *Robot. Comput.-Integr. Manuf.* **25**(2), 261–270 (2009a)
- Yildiz, A.R.: An effective hybrid immune-hill climbing optimization approach for solving design and manufacturing optimization problems in industry. *J. Mater. Process. Technol.* **209**(6), 2773–2780 (2009b)
- Yildiz, A.R.: A comparative study of population-based optimization algorithms for turning operations. *Inf. Sci.* **210**, 81–88 (2012)
- Yildiz, A.R.: Comparison of evolutionary-based optimization algorithms for structural design optimization. *Eng. Appl. Artif. Intell.* **26**(1), 327–333 (2013a)

- Yildiz, A.R.: A new hybrid differential evolution algorithm for the selection of optimal machining parameters in milling operations. *Appl. Soft Comput.* **13**(3), 1561–1566 (2013b)
- Yildiz, A.R.: A new hybrid artificial bee colony algorithm for robust optimal design and manufacturing. *Appl. Soft Comput.* **13**(5), 2906–2912 (2013c)
- Yildiz, A.R.: Optimization of cutting parameters in multi-pass turning using artificial bee colony-based approach. *Inf. Sci.* **220**, 399–407 (2013d)
- Yildiz, A.R.: Hybrid Taguchi-differential evolution algorithm for optimization of multi-pass turning operations. *Appl. Soft Comput.* **13**(3), 1433–1439 (2013e)
- Yildiz, A.R.: Cuckoo search algorithm for the selection of optimal machining parameters in milling operations. *Int. J. Adv. Manuf. Technol.* **64**(1–4), 55–61 (2013f)
- Zhang, C.-L., Shen, H.-S.: Thermal buckling of initially compressed single-walled carbon nanotubes by molecular dynamics simulation. *Carbon* **45**(13), 2614–2620 (2007)
- Zhang, Z., Guo, W., Dai, Y.: Freestanding (3,0) boron nitride nanotube: expected to be stable well over room temperature. *Appl. Phys. Lett.* **93**(22), 223108 (2008)
- Zhang, Z., Guo, W., Dai, Y.: Stability and electronic properties of small boron nitride nanotubes. *J. Appl. Phys.* **105**(8), 084312 (2009a)
- Zhang, Y.Y., Xiang, Y., Wang, C.M.: Buckling of defective carbon nanotubes. *J. Appl. Phys.* **106**(11), 113503 (2009b)